Reprinted from

CMES

Computer Modeling in Engineering & Sciences

Founder and Editor-in-Chief:
Satya N. Atluri

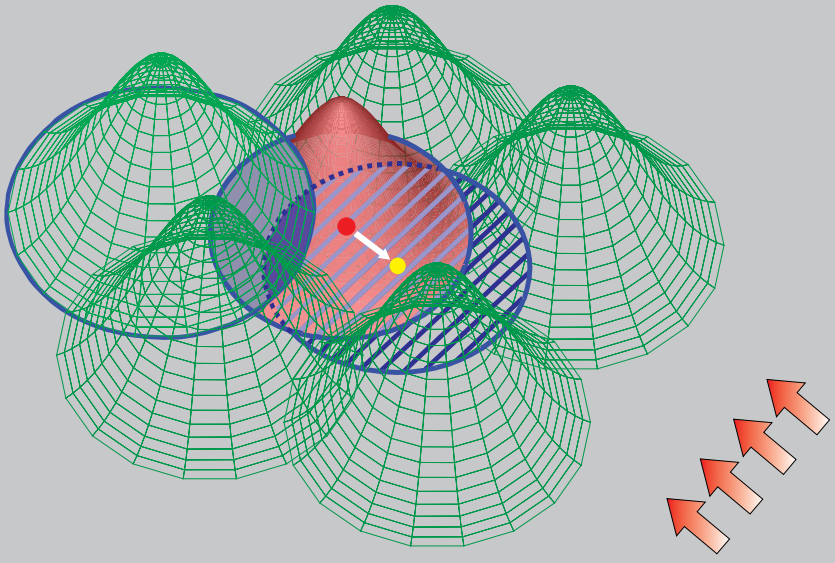

ISSN: 1526-1492 (print)
ISSN: 1526-1506 (on-line)

Tech Science Press

 CMES, vol.53, no.3, pp.235-254, 2009

Stable Manifolds of Saddles in Piecewise Smooth Systems

A. Colombo[1], **and U. Galvanetto** [2]

Abstract: The paper addresses the problem of computing the stable manifolds of equilibria and limit cycles of saddle type in piecewise smooth dynamical systems. All singular points that are generically present along one-dimensional or two-dimensional manifolds are classified and such a classification is then used to define a method for the numerical computation of the stable manifolds. Finally the proposed method is applied to the case of a stick-slip oscillator.

Keywords: basin of attraction, discontinuous, dynamical system, friction oscillator, numerical method, piecewise smooth, stable manifold

1 Introduction

In a smooth, linear, autonomous, and hyperbolic system, the eigenvectors of the system's matrix can be divided in two sets, one comprising all the stable eigenvectors and the other all the unstable ones. These sets span two invariant subspaces, commonly called the *stable* and *unstable manifolds*, containing all the initial conditions that converge to the equilibrium respectively forward or backward in time. An important result of nonlinear dynamics shows that a similar property holds true in the case of an equilibrium, or of a cycle, in a nonlinear system: consider the system linearised around the equilibrium or, in the case of a cycle, around the fixed point of a Poincaré map. As long as the equilibrium [fixed point] is hyperbolic, the nonlinear system is, locally, topologically equivalent to its linearisation. Then, sufficiently close to the equilibrium [fixed point] of the nonlinear system there exist two local invariant manifolds, tangent to the stable and unstable eigenspaces and of the same dimension as the respective eigenspaces, and the two manifolds can be continued, respectively backward and forward in time, to construct global invariant manifolds. The geometry of the global invariant manifolds can be remarkably complex and, in general, there is no way of computing them analytically; nonetheless, their study

[1] Department of Electronics and Information, Politecnico di Milano, Italy, email: alessandro.colombo@polimi.it
[2] Department of Structural and Transportation Engineering, Università di Padova, Italy.

can be a valuable tool in the analysis of the dynamics of a nonlinear system, since they act as organising sets for the system's orbits. They play a special role in the understanding of chaotic dynamics and, in the case of $(n-1)$-dimensional stable manifolds of saddle equilibria or cycles in n-dimensional systems, they mark the boundaries between different basins of attraction (for this reason, they are usually called *separatrices*).

The computation of invariant manifolds, and thus of basins of attraction, is not only of mathematical interest but might constitute a step in the design of a system of engineering relevance. Let us consider an engineering system in which multiple attractors coexist. Usually only one represents the normal functioning mode of the system, whereas the others are conditions to be avoided because the system cannot operate (safely) if it reaches them. The basin of attraction of the "safe state" is the set of all initial conditions that originate a transient attracted by the safe state itself. It is possible to define within the basin of attraction a "safety set" of all initial conditions which do not compromise the integrity of the system. Moreover another measure of the safety of the system might be provided by the distance between the attractor and its basin's boundaries, that would provide an indication of the size of the perturbation needed to bring the system out of the safe basin. Similar ideas have been proposed in the past, for example in (Soliman and Thompson, 1989; Thompson and Soliman, 1990).

These applications have motivated a number of studies, and recently a wealth of methods have been proposed to reconstruct invariant manifolds numerically (see (Krauskopf, Osinga, Doedel, Henderson, Guckenheimer, Vladimirsky, Dellnitz, and Junge, 2005) for a review). However, most of these results rely on the assumption that the vector field be sufficiently regular or, in other words, be smooth. When the smoothness assumption is relaxed, for example in the case of piecewise smooth systems that are used e.g., in models with friction or switches, things get more complicated: the sudden changes in the vector field generate corners in the invariant manifolds (which are, therefore, no longer smooth manifolds in the proper sense), and the presence of sliding makes the system's flow non-reversible. However, as we show in the following, not all the beautiful regularity of these manifolds is lost.

In this paper we discuss some properties of the stable manifolds of equilibria or cycles of saddle type in piecewise smooth systems, with particular attention to one- and two-dimensional manifolds. Our theoretical results apply to systems of any dimension but, as noted above, they are especially interesting in two- and three-dimensional systems, where stable manifolds separate basins of attraction. The paper is organised as follows: first, we spend a whole section to give a precise definition of piecewise smooth system, to set the basis for the following discussion;

then, we describe the topological properties of invariant manifolds and provide the full catalogue of the ways in which families of orbits in such manifolds can be affected by the discontinuities of the vector field; finally, we present a method to reconstruct numerically two-dimensional stable manifolds, and apply it to a realistic mechanical system. To obtain these results we inevitably make use of some rather subtle mathematical concepts, such as singular points or Lie derivatives, but we have made an effort to explain them as soon as they occur in the simplest possible way, in order to keep the reader's attention focused on the main matter of the paper.

2 Piecewise smooth systems

A piecewise smooth system is, roughly speaking, a dynamical system with a vector field that is smooth in regions of the state space, but discontinuous across the boundaries between such regions. More formally, it is defined as a system

$$\dot{x} = f(x), \quad x \in \mathbf{R}^n,$$

such that any finite open subset of the domain of $f(x)$ can be divided into a finite number of regions, and $f(x)$ is smooth in each region up to the boundary. Additionally, it is required that each finite open subset have common points with only a finite number of smooth regions. These systems were extensively studied by Filippov (1988) (while more recent results on their bifurcations are collected, e.g., in (Leine, 2000; Zhusubaliyev and Mosekilde, 2003; di Bernardo, Budd, Champneys, and Kowalczyk, 2008)), and their analysis was primarily motivated, at first, by applications in electrical and mechanical engineering, where switches or friction phenomena are quite naturally modelled as discontinuities in the vector field. In particular, in his famous book Filippov gave a definition of solutions at the surfaces of discontinuity (usually called *switching surfaces*), to cope with the fact that, there, the vector field may have different directions on the two sides of the surface. This definition is based on the concept of differential inclusion (Aubin and Cellina, 1984). It consists of considering any trajectory, whose time derivative belongs to the convex combination of the vector field on the two sides of the switching surface, to be a solution of the system. Thus, formally, if we consider a smooth portion of a switching surface, defined as the zero set of a scalar function

$$h(x) : \mathbf{R}^n \to \mathbf{R}, \tag{1}$$

and we assume that the vector field be locally equal to

$$\begin{cases} f^{(1)}(x) & \text{when} \quad h(x) > 0, \\ f^{(2)}(x) & \text{when} \quad h(x) < 0, \end{cases} \tag{2}$$

the vector field on the switching surface is

$$f^{(s)}(x) \in \lambda(x) f^{(1)}(x) + (1-\lambda(x)) f^{(2)}(x), \tag{3}$$

with $\lambda(x) \in [0,1]$. The same approach can be adapted, with little differences, to nonsmooth portions of the switching surface (see for example (Filippov, 1988)). Depending on the relative orientation of $f^{(1)}(x)$ and $f^{(2)}(x)$ with respect to the switching surface, the convex set in (3) may or may not contain components along the switching surface: when both vector fields point towards or away from the switching surface, so that

$$\sigma(x) := \mathscr{L}_{f^{(1)}} h(x) \mathscr{L}_{f^{(2)}} h(x) < 0, \tag{4}$$

then their convex combination includes a component along the switching surface, while this is not the case when $\sigma(x) > 0$. In the formula above, $\mathscr{L}_{f^{(i)}} h(x)$ is the Lie derivative of $h(x)$ along the direction of $f^{(i)}(x)$ or, in other words, the scalar product of $f^{(i)}$ and the gradient of h evaluated at x. Regions of the switching surface where $\sigma(x) < 0$ are called *sliding regions* when neighbouring orbits converge to the surface or *escaping regions* when they diverge, while regions where $\sigma(x) > 0$ are called *crossing regions*. Thus, points where $\sigma(x) = 0$, where either $f^{(1)}(x)$ or $f^{(2)}(x)$ is tangent to the switching surface, mark the boundaries between crossing regions and sliding or escaping regions. A point of tangency where orbits are curved away from the switching surface is called a *visible* tangency point, while it is an *invisible* tangency point when orbits are curved toward the surface. When a segment of orbit of $f^{(1)}(x)$ or $f^{(2)}(x)$, called a *regular* segment, reaches a sliding or escaping region (in finite time, respectively forward or backward in time), the orbit is then constrained to "slide", following the component of (3) tangent to the switching surface. The segment of orbit on the surface is called accordingly a *sliding* or *escaping* segment. In crossing regions, orbits that reach the switching surface simply cross it, and continue on the other side. The most important consequence of this definition is that piecewise smooth systems admit multiple solutions, backward in time in the sliding regions and forward in time in the escaping regions. This contrasts with the case of smooth vector fields, which under very mild assumptions admit unique solutions both forward and backward in time.

3 Topology of a stable manifold in a piecewise smooth system

The shape of the global stable manifolds of a saddle cycle or equilibrium in continuous time systems can be extremely complex to describe, let alone to compute numerically, but as long as we constrain our attention to smooth systems, and to finite subsets of the stable manifold, these sets are relatively well behaved: technically, they are embedded smooth manifolds in the system's state space (see e.g,

(Meiss, 2007) for some details in this regard). In layman's terms, this means that any finite subset of the stable manifold is obtained by immerging a hypersurface of the appropriate dimension in the state space, without pinching it, cutting it, or causing it to self-intersect. Unfortunately, the same is not true in the case of piecewise smooth systems: the discontinuities of the vector field can affect the shape of the manifold. However, far away from the switching boundaries the manifold is still generated by a smooth flow, so that all creases originate at the intersection of the manifold with the switching surface. To understand the geometries of these intersections, we can exploit some of the results of catastrophe theory, as it was developed by Whitney (1955) and Thom (1975) (and explained nicely by Poston and Stewart (1978)). This theory has been succesfully used to analyse many physical systems (for a recent example, see (Cui, Liao, and Yu, 2009), while many more are found in the second part of Poston's book). In the domain of piecewise smooth dynamical systems, its has been exploited in Jeffrey and Hogan (submitted) for the analysis of slding bifurcations, as a systematic way of classifying the geometries of two intersecting surfaces. We follow a similar approach in this paper, and the results that we list hereafter are simple consequences of the theorems contained in the references above. All the results that follow are obtained assuming a smooth switching surface, but can easily be extended to the nonsmooth case.

Oversimplifying, catastrophe theory classifies the ways in which maxima and minima of a function $V(t,p)$, t and p being respectively vectors of variables and parameters, can collide and annihilate when some parameters are changed. Points in the space (t,p) where two or more of these points collide are called *singular* points. In the context of our analysis, we only need to consider the relatively simple case of $t \in \mathbf{R}$ and, rather than considering maxima and minima of $V(t,p)$ we look at the zeros of

$$\frac{dV(t,p)}{dt}. \tag{5}$$

For a fixed value of p, function (5) has, generically, only simple isolated zeros, at points where it crosses the horizontal axis transversely. In the jargon of catastrophe theory these are called *Morse* points, while those where (5) is nonzero are *regular* points. All other types of intersection with the horizontal axis, like quadratic or cubic tangencies, are *structurally unstable*, in that they decompose into a number of Morse points when the function is perturbed. However, if we consider a one-parameter family of functions, that is, if we allow one of the components of vector p to change over an interval, then generic members of the family will have only regular and Morse points, but isolated members may intersect the horizontal axis quadratically, at so called *fold* points. Similarly, if we allow p to change along two directions, regular, Morse and fold points become generic, but higher order singular

points arise, namely cubic tangencies or *cusp* points appear in isolated members of the family. Proceeding along this line, one can classify the type of singular points that can be found in larger families of functions.

Since a stable manifold is a set of orbits converging toward a given invariant set, by representing the manifold as a family of functions, assigning to each segment of orbit, regular, sliding or escaping, a function like (5) that goes to zero when the orbit crosses the switching surface, we can rely on the results of catastrophe theory to classify the intersections of the manifold with the switching surface, and to identify the singular points along the manifold. To proceed, we first need to find a suitable function (5). Consider a generic n-dimensional system with a smooth switching surface defined as in (1) and vector field defined as in (2), and a saddle invariant set with an m-dimensional stable manifold. Choosing an $(m-1)$-dimensional subset

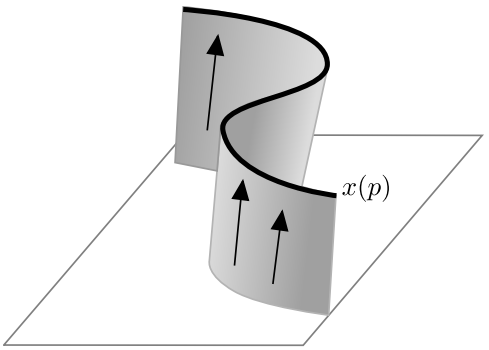

Figure 1: The one-dimensional set $x(p)$ (in black) intersects transversely all the orbits lying in a portion of the stable manifold (in grey).

$x(p)$ of the stable manifold, with $p \in \mathbf{R}^{m-1}$, that intersects transversely the system's orbits as in Fig. 1, we can write segments of orbits intersecting $x(p)$ locally in terms of the flow of points in $x(p)$ under the vector fields $f^{(1)}(x)$, $f^{(2)}(x)$, or $f^{(s)}(x)$, that is,

$$\phi^{(1)}(t,x(p)), \tag{6a}$$

$$\phi^{(2)}(t,x(p)), \tag{6b}$$

$$\phi^{(s)}(t,x(p)), \tag{6c}$$

for $t \in \mathbf{R}$. Equations (6a) and (6b) define regular segments, while eq. (6c) defines sliding or escaping segments in the switching surface. Given the definitions of the functions $h(x)$ and $\sigma(x)$ provided in (1) and (4), the intersections of these segments

with the switching surface, or with the boundaries of the sliding or escaping regions correspond to the zero sets of

$$h(\phi^{(1)}(t,x(p))), \tag{7a}$$
$$h(\phi^{(2)}(t,x(p))), \tag{7b}$$
$$\sigma(\phi^{(s)}(t,x(p))). \tag{7c}$$

These are $(m-1)$-parameter families of functions, from $\mathbf{R}$ to itself, in the parameters p and in the variable t, just as we needed.

Having set up a framework of analysis, we are now ready to classify the intersections of a stable manifold with the switching surface. We focus in particular on one- and two-dimensional manifolds, which are easy to visualise and can be computed through efficient numerical algorithms, but the same procedure can in principle be extended to higher dimensional manifolds. Let us start by observing what can happen along a one-dimensional stable manifold. At an intersection with a crossing region of the switching surface, taking $x(p)$, with p fixed, to be the intersection point, two segments of orbit, described by equations (6a) and (6b) emanate from the crossing point, which is a zero of both (7a) and (7b). As we have seen, these are generically Morse points, where $h(\phi^{(1,2)}(t,x(p)))$ crosses 0 transversely as t is changed around 0. Therefore, generically the two segments meet the switching surface transversely, as in Fig. 2a. A similar reasoning holds when the stable manifold intersects an escaping region, by substituting one of the flows with the sliding flow (6c), and the corresponding function (7a) or (7b) with (7c). In this case, the intersection point is Morse for (7a) or (7b), while it is a regular point of (7c), as in Fig. 2b. Notice that a one-dimensional stable manifold can intersect an escaping region, but generically does not intersect a sliding region, since that would imply that a sliding segment, and all the regular segments terminating on it, belong to the manifold, which would therefore be two-dimensional. When an escaping segment of the stable manifold intersects the border of an escaping region at a point $x(p)$, this is in general a Morse point of (7c), but, by the definition of σ, it is a fold of either (7a) or (7b), that is, a quadratic tangency of either $\phi^{(1)}(t,x)$ or $\phi^{(2)}(t,x)$, as in Fig. 2c. The intersections of a one-dimensional manifold with the switching surface therefore generically occur in one of the three scenarios depicted in Fig. 2, and the stable manifold is, locally, a "piecewise smooth manifold", in that it consists of smooth segments pieced together at a nonzero angle.

We can now analyse the case of two-dimensional manifolds by allowing p to change along a single direction, thus generating a one-parameter family of functions. Since each member of the family is a one-dimensional manifold, our conclusions for the previous case must still hold for a generic member of the one-parameter family. However, as we have seen above, isolated members of the family can contain higher

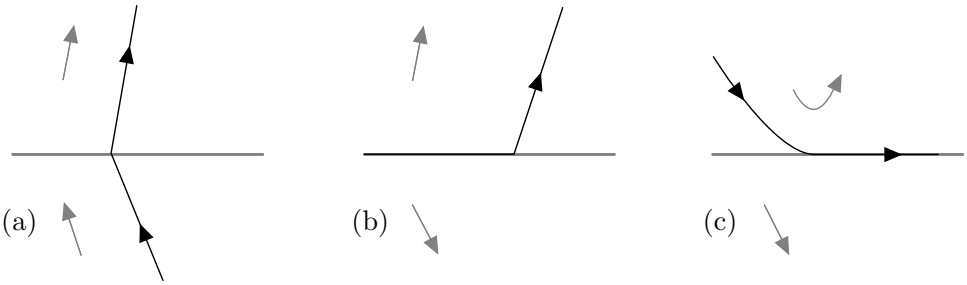

Figure 2: The intersection of a one-dimensional manifold (black) with a switching surface (grey) generically occurs in one of the three scenarios above: two regular segments transversely intersect the switching surface (a); a regular segment emerges from an escaping region, the escaping segment being part of the manifold up to the intersection with the regular segment (b); a regular segment intersects the switching manifold tangentially, and the orbit continues into an escaping segment (c). In the figure, arrows on the orbits indicate the positive direction of time, while grey arrows sketch the vector field above and below the switching surface.

order singular points. Take a portion of the manifold that lies, for example in the region where $h(x) > 0$, where according to (2) orbits follow the vector field $f^{(1)}(x)$, and a one-parameter family of initial conditions $x(p)$ that intersects transversely all the regular segments in this portion. If these segments, followed back in time, intersect the switching surface, then almost all points along the intersection are Morse points of both (7a) and (7b), but we can expect to find four kinds of isolated fold points, giving place to the four portraits in Fig. 3. These can be visible quadratic tangencies of $f^{(1)}(x)$, with $f^{(2)}(x)$ (a) diverging from or (b) converging to the switching surface, or (c) visible or (d) invisible quadratic tangencies of $f^{(2)}(x)$. More precisely:

In Fig. 3a, a segment of $f^{(1)}(x)$ is visibly tangent to the switching surface, while $f^{(2)}(x)$ points away from the surface, so that the stable manifold lies locally on one side of the switching surface, sliding on it in an escaping region. Orbits that comprise an escaping segment reach the switching surface as in Fig. 2c and leave it as in Fig. 2b.

In Fig. 3b, a segment of $f^{(1)}(x)$ is visibly tangent to the switching surface, but $f^{(2)}(x)$ points toward the switching surface. This implies that a sliding segment terminates at the fold point, hence, while sliding segments cannot be part of a one-dimensional manifold, isolated sliding segments can belong to a two-dimensional one.

In Fig. 3c, a segment of $f^{(2)}(x)$ reaches the switching surface tangentially, and then

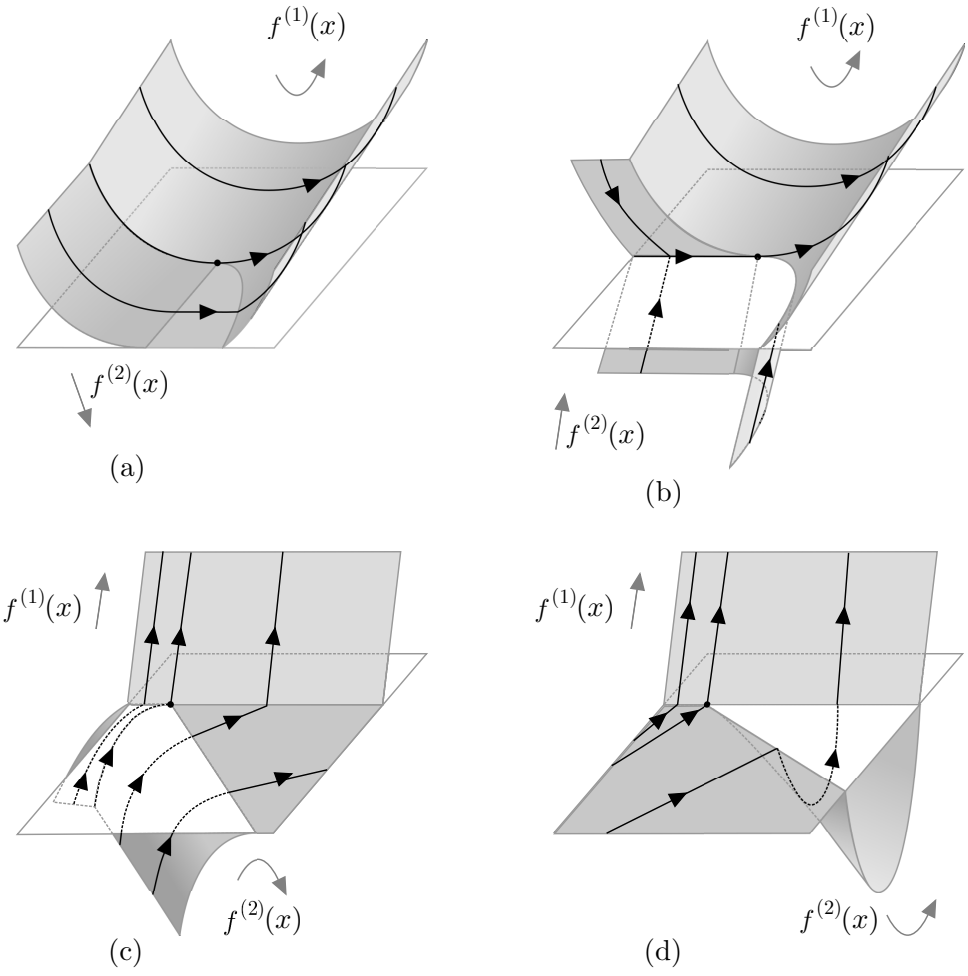

Figure 3: Geometry of the stable manifold (grey surface) at the intersection with the switching surface (white) around a fold point (black dot). In (a), (c), and (d) part of the stable manifold lies in an escaping region of the switching surface, while in (b) a sliding segment belongs to the stable manifold. As in Fig. 2, arrows on the orbits indicate the positive direction of time, while grey arrows sketch the vector field above and below the switching surface.

crosses to the other side. Nearby orbits thus either cross the switching surface (as in Fig. 2a), or slide in an escaping region before crossing (undergoing the scenarios in Fig. 2c and then b).

Finally, in Fig. 3d, a segment of $f^{(2)}(x)$ is invisibly tangent to the switching surface,

so that orbits reaching a neighbourhood of this fold point along the escaping region either leave the switching surface directly along the field $f^{(1)}(x)$, as in Fig. 2b, or along the field $f^{(2)}(x)$, crossing the switching surface shortly afterwards, (scenarios in Fig. 2b and then Fig. 2a). Notice that scenarios a,b, and c generically imply that a crease of the stable manifold extends away from the switching surface, while in the scenario d the manifold is locally smooth away from the switching surface.

The four scenarios above regard isolated singularities that can be found generically along a family of regular segments. Considering isolated sliding segments or families of escaping segments, we can identify four more scenarios. Following a sliding orbit backward in time, this can reach a boundary of the sliding region, at a fold point of either (7a) or (7b), giving place to the portrait in Fig. 4. If we follow a

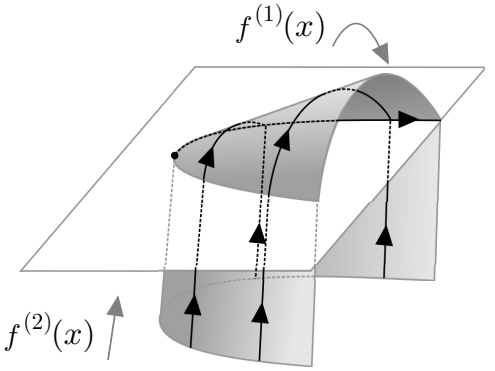

Figure 4: Stable manifold around a fold of a sliding segment. Surfaces and arrows have the same meaning as in Fig. 3

family of escaping segments backward in time, these generically leave the switching surface through fold points of (7a) or (7b), but isolated cusps of either (7a) or (7b), or simultaneous folds of both (7a) and (7b), called *two-fold* singularities, can be encountered. In the first case, the manifold is locally equivalent to that in Fig. 5. Notice that, like in Fig. 3, in Fig. 4 and Fig. 5 the stable manifold is creased only along the switching surface, and smooth elsewhere. The second case is more complex: dynamics around a two-fold have been investigated for some time (Filippov, 1988; Teixeira, 1990, 1993), but the subtle nonlinear dynamics surrounding these points have started to be understood only recently (Jeffrey and Colombo, 2009), and are the subject of ongoing research. In these papers, the geometry of the orbits around the two-fold singularity have been shown to change dramatically from the case where both vector fields are visibly tangent to the switching surface to those where at least one is invisibly tangent. The scenario depicted in Fig. 6 ($f^{(1,2)}$ both

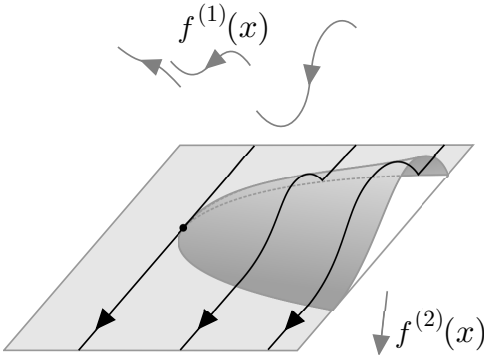

Figure 5: Stable manifold around a cusp point. Surfaces and arrows have the same meaning as in Fig. 3. The black dot is a cusp point of $f^{(1)}(x)$.

visibly tangent to the switching surface) is relatively straightforward, and always preserves the manifold structure around the singular points. The other scenarios are much more difficult to analyse since the invisible tangency can cause an infinite number of orbits to converge toward the singular point in finite time, and in the worst, double invisible case, may also make the orbits, and thus the manifold, wind around the singularity. While an introduction to these intricate dynamics is given in the cited references, deeper understanding is needed to discuss the structure of an invariant manifold around such two-fold points in the general setting.

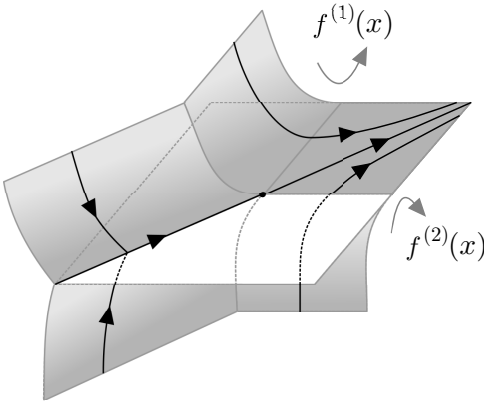

Figure 6: Stable manifold around a two-fold point, when both $f^{(1)}(x)$ and $f^{(2)}(x)$ are visibly tangent to the switching surface. Surfaces and arrows have the same meaning as in Fig. 3. The black dot is a fold point of both vector fields.

4 Numerical computation of the stable manifold

The analysis conducted in the previous section classifies all the singular points that are generically present along a one- or two-dimensional manifold. While the computation of a one-dimensional manifold is trivial, requiring just to follow an orbit back in time, and through all its intersections with the switching manifold, in this section we propose a method to reconstruct numerically a two-dimensional stable manifold. Our method is based on that proposed, for smooth manifolds, by Doedel in (Krauskopf, Osinga, Doedel, Henderson, Guckenheimer, Vladimirsky, Dellnitz, and Junge, 2005), complemented with the classification above.

Dodel's method consists in reconstructing a smooth two-dimensional stable manifold by numerically continuing an orbit of the manifold as its end point is moved and, typically, the one-parameter family of end points is chosen in the linear approximation of the manifold around the invariant set. This method is easily implemented as a boundary value problem, where the boundary conditions are the endpoint, plus a suitably chosen condition setting the length of the orbits, e.g. their time length or arclength. The boundary value problem is then solved numerically using continuation software such as AUTO (Doedel, Champneys, Dercole, Fairgrieve, Kuznetsov, Oldeman, Paffenroth, Sandstede, Wang, and Zhang, 2007) (see the reference above for all details).

This method is easily adapted to the continuation of an orbit of a piecewise smooth system, simply by setting up a boundary value problem for each smooth segment of the orbit, and imposing that the endpoints of all segments, except the first and the last, match. Once the sequence of segments composing the orbit is known, the orbit continuation is carried out exactly as in the smooth case. This is the philosophy behind the continuation software TC-HAT (Thota and Dankowicz, 2008), a modified version of AUTO written to handle discontinuous systems, which we have used to obtain the results in the following section. However, the sequence of smooth segments that constitutes an orbit may (and in general does) change as the orbit spans the invariant manifold. It happens precisely when the orbit intersects one of the seven singular points that are listed in Sec. 3, and the occurrence of these transitions, and their nature, is easily determined by monitoring the intersections of the orbits' segments with the switching surface. Considering that the labels $f^{(1)}(x)$ and $f^{(2)}(x)$ can be assigned in two ways to the vector fields on the sides of the switching surface, and assuming a positive value of $h(x)$ where $f^{(1)}(x)$ is defined (as we did above), any singular point $\bar{x}$ satisfies exactly one of the seven sets of conditions in Tab 1 for one of the two choices of vector label (or equivalently, it satisfies one of the sets of conditions in Tab 1, or one obtained by swapping $f^{(1)}(x)$ and $f^{(2)}(x)$ in the table, and reversing all inequalities). Notice that the conditions for Fig. 3a and c are equivalent when swapping the vector fields' labels, but the two scenarios can be

scenario	$\mathscr{L}_{f^{(1)}}h(\bar{x})$	$\mathscr{L}^2_{f^{(1)}}h(\bar{x})$	$\mathscr{L}_{f^{(2)}}h(\bar{x})$	$\mathscr{L}^2_{f^{(2)}}h(\bar{x})$
Fig. 3a	0	>0	<0	
Fig. 3b	0	>0	>0	
Fig. 3c	>0		0	<0
Fig. 3d	>0		0	>0
Fig. 4	0	<0	>0	
Fig. 5	0	0	<0	
two-fold	0		0	

Table 1: Conditions for the seven singular points identified in Sec. 3. When a condition is not specified, the corresponding value is indifferent.

distinguished, for example, by imposing that the orbit emerging from the singular point belong to a specific vector field (e.g. $f^{(1)}(x)$). These singular point conditions can thus be checked systematically, to determine the type of transition, and deduce how the sequence of segments that constitute the orbit changes past the singular point. Notice that the occurrence of case 3b not only signals a change in the orbit's sequence of segments, but also the presence of a sliding segment terminating on the singular point. This sliding segment is in turn the terminal set of a family of segments that, again, belong to the stable manifold.

5 Application to a sliding block model

We now use the results in the previous sections to study a periodically forced dry friction system first proposed in (Oestreich, Hinrichs, and Popp, 1996; Galvanetto, 2008), consisting of a block of mass m laying on a belt that moves with constant velocity V_{dr}. The block is attached to a linear spring of stiffness k and rest position $x_1 = 0$, and is subject to a periodically varying force of magnitude a and frequency w, while the friction law is chosen equal to

$$\mu_k = \frac{\alpha}{1+\gamma|x_2 - V_{dr}|} + \beta + \eta(x_2 - V_{dr})^2,$$

where $x_2 = \dot{x}_1$ is the velocity of the block. The law of motion when the block is slipping is

$$m\dot{x}_2 = -kx_1 + a\cos(wt) + \mu_k mg,$$

and adopting the formalism of Sec. 2, we can rewrite the system as

$$h(x) = x_2 - V_{dr}$$

and

$$\begin{aligned} f^{(1)}(x) &= \left(\frac{-kx_1 + a\cos(wt)}{m} - g\left(\frac{x_2}{1+\gamma(x_2 - V_{dr})} + \beta + \eta(x_2 - V_{dr})^2 \right) \right), \\ f^{(2)}(x) &= \left(\frac{-kx_1 + a\cos(wt)}{m} + g\left(\frac{x_2}{1-\gamma(x_2 - V_{dr})} + \beta + \eta(x_2 - V_{dr})^2 \right) \right). \end{aligned} \tag{8}$$

Since the friction force depends discontinuously on the sign of $x_2 - V_{dr}$, this is a three-dimensional piecewise smooth systems in the variables t, x_1, and x_2.

This model was analysed in (Galvanetto, 2008) for the parameter values

$$m = 1, \quad k = 1, \quad a = 3.6, \quad w = 1.067, \quad g = 10,$$
$$V_{dr} = 1, \quad \alpha = 0.3, \quad \beta = 0.1, \quad \gamma = 1.42, \quad \eta = 0.01.$$

There, it was shown to have two stable limit cycles and a saddle one (respectively in green and red in Fig. 7) of period $2\pi/w \simeq 5.8886$,

the stable manifold of the saddle cycle separating the basins of attraction of the two stable cycles, and the intersection of this stable manifold with the surface $t = 0$ was reconstructed numerically, obtaining the plot in Fig. 8.

Using the results and methods explained in the previous sections, we were able to reconstruct this manifold in the full three-dimensional space (t, x_1, x_2). Since the saddle cycle has (two) sliding segments, all the orbits of its stable manifold must eventually converge to one of these segments, which were therefore chosen as the families of end points to generate the whole manifold. Then, to keep the size of the manifold's surface finite, orbits that depart from the sliding segments were plotted only up to their first intersection (backward in time) with the surfaces $x_2 = \pm 5$ (chosen arbitrarily). The resulting surface is plotted in Fig. 9, together with the stable (green) and saddle (red) cycles.

Looking at the behaviour of the vector field of (8) near the switching surface $x_2 = V_{dr}$, it is easy to show that the surface has two crossing regions and a sliding region, but no escaping regions, as frequently happens in friction models. As a consequence, of the seven singular points that we have classified in Sec. 3, only those in Fig. 3b and 4 can occur in this system, since the others imply the presence of an escaping region near the singular point. In particular, as we have seen above, these two points must appear in couples as initial and terminal point of each sliding segment belonging to the manifold. We identified three such segments (and thus six singular points), two that contain the sliding segments of the cycle as their terminal

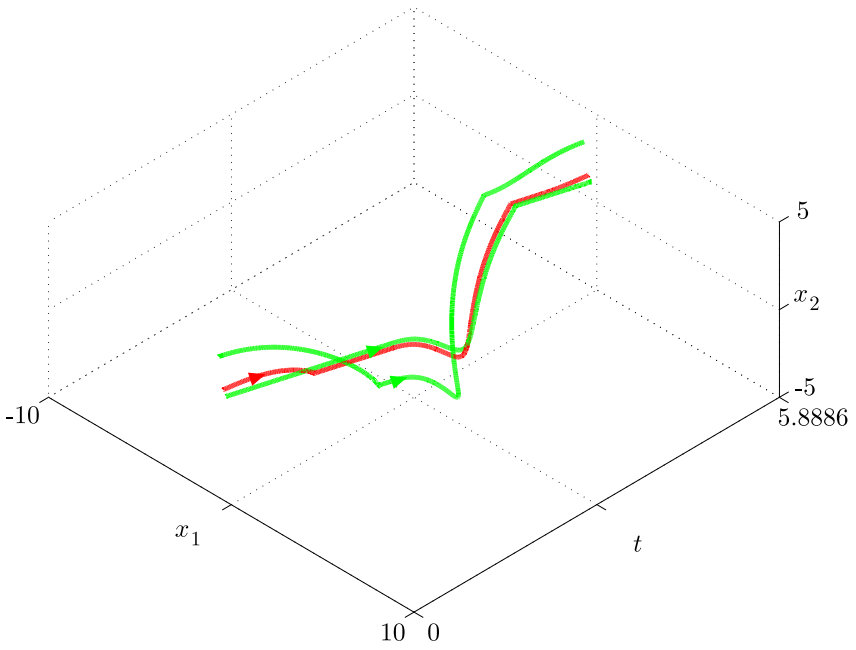

Figure 7: The saddle cycle (red) and the two stable cycles (green). The yellow dot is a singular point of the stable manifold of the saddle cycle (see Fig.10).

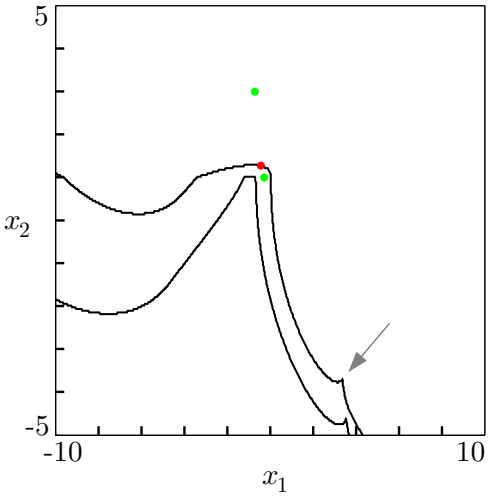

Figure 8: Boundary of the basins of attraction of the two stable cycles on the surface $t = 0$. The intersections of the stable and saddle cycles with the figure's plane are represented respectively as green and red dots. The arrow indicates a corner of the basin's boundaries, corresponding to a crease of the stable manifold visible in Fig.9.

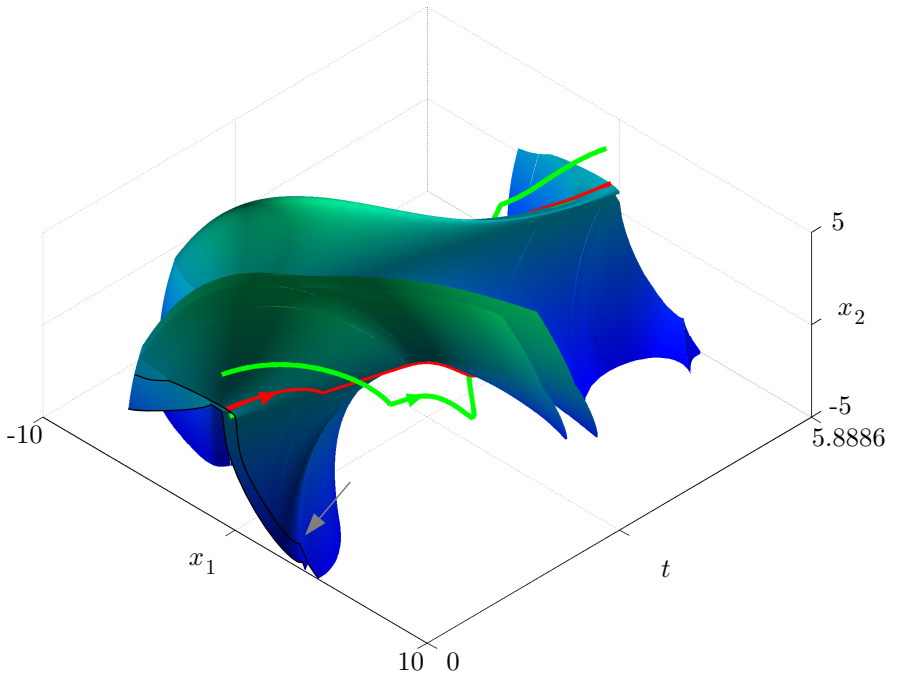

Figure 9: The blue surface is the stable manifold of the saddle cycle. Orbits of the manifold were continued backward in time up to their first intersection with the surfaces $x_2 = \pm 5$. The red and green cycles are respectively the saddle cycle and the two stable ones. The intersection of the stable manifold with the plane $t = 0$, plotted here in black, correspond to the boundary represented in Fig. 8. Part of the boundary appearing in Fig. 8 is not shown in this figure, since it is generated by orbits that extend beyond the interval $x_2 \in [-5, +5]$. The arrow in the lower left part of the figure indicates the crease mentioned in Fig.8.

part, and one which does not intersect the cycle. One of these segments is represented in yellow in Fig. 10. It is a straight line on the plane $x_2 = 1$, appearing as two separate segments in the figure because it spans more than one period. Notice that, as predicted, the manifold has a crease departing from the leftmost singular point, which is visible in the lower part of Fig. 9 and 10, and explains one of the corners observed along manifold's section in Fig. 8 (the other one is due to another singular point of the same type). Having the complete surface it is now a simple task to estimate the euclidean distance of each of the stable cycles from the manifold, useful to estimate their resilience to perturbation, simply by determining the distance between the set of points constituting each cycle, and that constituting the

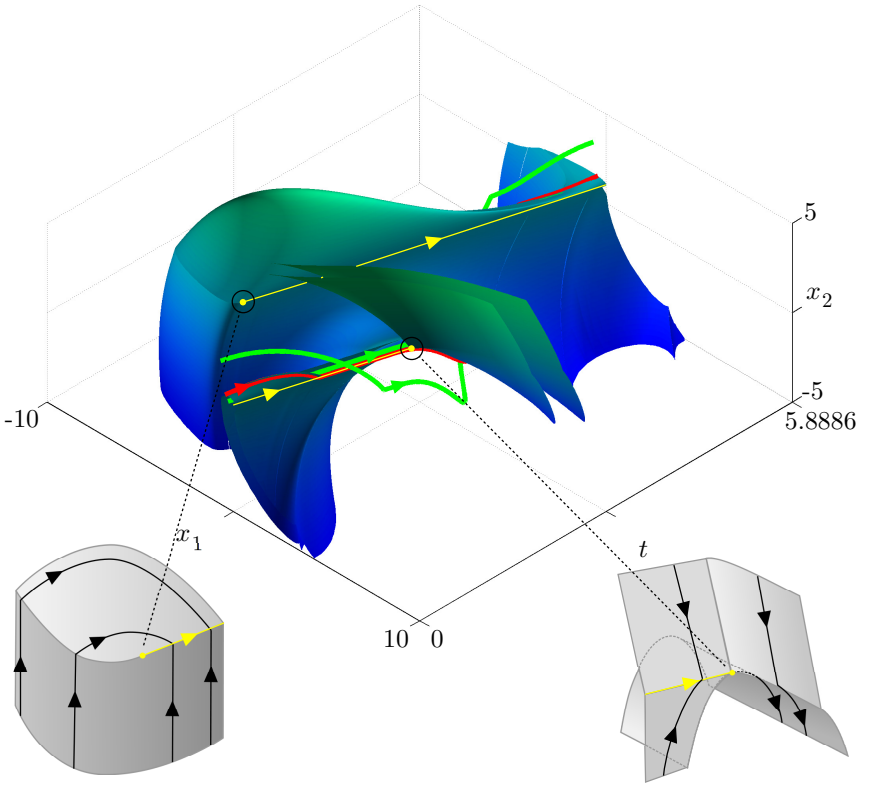

Figure 10: The stable manifold contains three isolated sliding segments, delimited by singular points as in Fig. 3b and 4. Here, one of the sliding segments and the two singular points delimiting it are highlighted in yellow, and the manifold's geometry around the two singular points is sketched. The singular point on the right lies on the saddle cycle (red). Part of the stable manifold has been removed to expose the singular point on the left.

manifold's surface. The resulting distances were found to be approximately 0.57 (for the cycle "outside" the manifold) and 0.05 (for the one "inside" the manifold), much smaller than those measurable from Fig. 8, which are approximately equal to 1.68 and 0.24 respectively. These values provide an estimate of the maximum (isolated) perturbation that the system can withstand without changing attractor, as shown in Fig. 11.

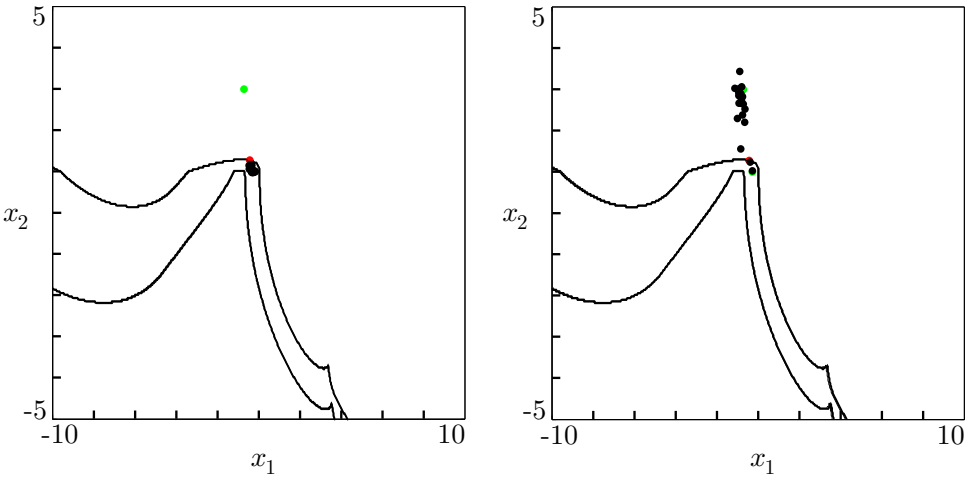

Figure 11: Iterations of the Poincaré' map of perturbed systems. A random vector perturbation of length uniformely distributed between 0 and 0.02 (left) or 0.06 (right) was added to the state variables x_1 and x_2 at regular intervals, once every 0.058886 unit times. In the left, the perturbed orbit remains strictly inside a basin of attraction, while on the right it crosses the basin's boundary an converges to a different attractor. Notice that, though the minimal distance of the inner cycle from the basin's boundary is approximately 0.05, smaller but frequent perturbations can add up and push the orbit outside the basin.

6 Conclusions

We have classified the complete set of singular points that appear generically along one- and two-dimensional stable manifolds in piecewise smooth systems, while providing a way to extend, at least in principle, this classification to higher dimensional manifolds. This classification allows us to explain the geometry of such manifolds, which turn out to be continuous (but not differentiable) surfaces, near all but one singular points. Additionally, it provides a practical way to reconstruct numerically the manifolds, with the help of existing software. The results and methods developed in the paper were then used to reconstruct the stable manifold of a saddle cycle in a dry friction model.

References

Aubin, J. P.; Cellina, A. (1984): *Differential Inclusions*. Springer-Verlag, Berlin.

Cui, T.; Liao, W.; Yu, D. (2009): Topological approach for analyszing and modeling the aerodynamic hysteresis of an airfoil. *CMES: Computer Modeling in*

Engineering & Sciences, vol. 45, pp. 273–293.

di Bernardo, M.; Budd, C. J.; Champneys, A. R.; Kowalczyk, P. (2008): *Piecewise-smooth Dynamical Systems: Theory and Applications*. Springer-Verlag.

Doedel, E. J.; Champneys, A. R.; Dercole, F.; Fairgrieve, T. F.; Kuznetsov, Yu. A.; Oldeman, B.; Paffenroth, R. C.; Sandstede, B.; Wang, X. J.; Zhang, C. H. (2007): AUTO-07p: Continuation and bifurcation software for ordinary differential equations. Department of Computer Science, Concordia University, Montreal, QC, 2007.

Filippov, A. F. (1988): *Differential Equations with Discontinuous Righthand Sides*. Kluwer Academic Publishers, Dordrecht.

Galvanetto, U. (2008): Computation of the separatrix of basins of attraction in a non-smooth dynamical system. *Physica D*, vol. 237, pp. 2263–2271.

Jeffrey, M. R.; Colombo, A. (2009): The two-fold singularity of discontinuous vector fields. *SIAM Journal on Applied Dynamical Systems*, vol. 8, pp. 624–640.

Jeffrey, M. R.; Hogan, S. J. (submitted): The geometry of generic sliding bifurcations. *SIAM Review*. Online preprint: http://seis.bris.ac.uk/ mm0093/SIREV2009

Krauskopf, B.; Osinga, H. M.; Doedel, E. J.; Henderson, M. E.; Guckenheimer, J.; Vladimirsky, A.; Dellnitz, M.; Junge, O. (2005): A survey of methods for computing (un)stable manifolds of vector fields. *International Journal of Bifurcation and Chaos*, vol. 15, pp. 763–791.

Leine, R. I. (2000): *Bifurcations in Discontinuous Mechanical Systems of Filippov-Type*. Ph.D. thesis, Technical University of Eindhoven, 2000.

Meiss, J. D. (2007): *Differential Dynamical Systems*. SIAM.

Oestreich, M.; Hinrichs, N.; Popp, K. (1996): Bifurcation and stability analysis for a non-smooth friction oscillator. *Archive of Applied Mechanics*, vol. 66, pp. 301–314.

Poston, T.; Stewart, I. (1978): *Catastrophe Theory and its Applications*. Pitman.

Soliman, M. S.; Thompson, J. M. T. (1989): Integrity measures quantifying the erosion of smooth and fractal basins of attraction. *Journal of Sound and Vibration*, vol. 135, pp. 453–475.

Teixeira, M. A. (1990): Stability conditions for discontinuous vector fields. *Journal of Differential Equations*, vol. 88, pp. 15–29.

Teixeira, M. A. (1993): Generic bifurcation of sliding vector fields. *Journal of Mathematical Analysis and Applications*, vol. 176, pp. 436–457.

Thom, R. (1975): *Structural Stability and Morphogenesis*. Benjamin, Reading, MA. (translated by D. H. Fowler).

Thompson, J. M. T.; Soliman, M. S. (1990): Fractal control boundaries of driven oscillators and their relevance to safe engineering design. *Proceedings of the Royal Society of London* A, vol. 428, pp. 1–13.

Thota, P.; Dankowicz, H. (2008): TC-HAT ($\widehat{TC}$): A novel toolbox for the continuation of periodic trajectories in hybrid dynamical systems. *SIAM Journal on Applied Dynamical Systems*, vol. 7, pp. 1283–1322.

Whitney, H. (1955): On singularities of mappings of Euclidean spaces 1. mappings of the plane into the plane. *Annals of Mathematics*, vol. 62, pp. 374–410.

Zhusubaliyev, Z. T.; Mosekilde, E. (2003): *Bifurcations and Chaos in Piecewise-Smooth Dynamical Systems*. World Scientific.

CMES: Computer Modeling in Engineering & Sciences

ISSN : 1526-1492 (Print); 1526-1506 (Online)

Journal website:
http://www.techscience.com/cmes/

Manuscript submission
http://submission.techscience.com

Published by
Tech Science Press
5805 State Bridge Rd, Suite G108
Duluth, GA 30097-8220, USA

Phone (+1) 678-392-3292
Fax (+1) 678-922-2259
Email: sale@techscience.com
Website: http://www.techscience.com
Subscription: http://order.techscience.com

CMES is Indexed & Abstracted in
Applied Mechanics Reviews; Cambridge Scientific Abstracts (Aerospace and High Technology; Materials Sciences & Engineering; and Computer & Information Systems Abstracts Database); CompuMath Citation Index; Current Contents: Engineering, Computing & Technology; Engineering Index (Compendex); INSPEC Databases; Mathematical Reviews; MathSci Net; Mechanics; Science Alert; Science Citation Index; Science Navigator; Zentralblatt fur Mathematik.